

Numerical Prediction of Wave Drag of 2-D and 3-D Bodies under or on a Free Surface

Yasin USLU

Delta Marine Design and Consultancy Company, İstanbul-TURKEY

Şakir BAL

İstanbul Technical University, Department of Naval Architecture and Marine Engineering

İstanbul-TURKEY

e-mail: sbal@itu.edu.tr

Received 05.02.2008

Abstract

The flow characteristics such as; wave drag, lift (if present in the case of 2-D), wave pattern, and pressure distribution around 2-D and 3-D bodies moving steadily under or on a free surface are investigated by 2 different boundary element methods. The iterative boundary element method (IBEM), which was originally developed for both 2-D and 3-D cavitating hydrofoils and ship-like bodies moving with constant speed under or on the free surface, is applied here in the case of a 2-D hydrofoil with an angle of attack, and some extended results are given. The effects of Froude number and the depth of submergence of hydrofoil from the free surface on pressure distribution and lift and wave drag values and the free surface wave elevation are discussed. The original method of Dawson, on the other hand, is applied to predict the wave pattern and wave drag values of fully submerged bodies (submarine) or surface piercing bodies (ship hull) in the case of 3-D. Some extensive numerical results are also shown to compare with those of experiments and other numerical methods in the literature.

Key words: Ship wave pattern, Wave drag, Free surface, Boundary element method, Hydrofoil

Introduction

Numerical prediction of wave pattern, wave drag, and pressure distribution around 2-D and 3-D bodies such as; ships, submarines, and hydrofoils moving with constant speed is very important for naval, marine, and ocean engineers and designers. The steady-state characteristics of flow around both fully submerged hydrofoils in the case of 2-D and surface piercing (ship-like hulls) bodies or fully submerged (submarine-like) bodies in the case of 3-D are addressed in this paper. The iterative boundary element method (IBEM) developed originally for submerged 2-D and 3-D cavitating hydrofoils moving with a constant speed under a free surface is applied to a 2-D hydrofoil with an angle of attack and the original method of Dawson for fully submerged 3-

D bodies (submarine type of bodies) or 3-D surface piercing (ship-like) bodies is applied to an ellipsoid and a mathematical Wigley form, and some extended numerical results are shown to compare with those of experimental measurements and other numerical methods.

Theoretical wave pattern and wave drag (resistance) were reviewed by Wehausen (1973) and Newman (1977) in the past. More recently, current trends of ship hydrodynamics including wave drag (resistance) in calm water were reviewed in Bulgarelli et al. (2003). On the other hand, some historical perspectives and reflections of ship waves were given by Tulin (2005). There are 2 groups of boundary integral methods for predicting ship wave drag; Kelvin wave source and Rankine source. Two different Kelvin source methods for 2-D hydrofoils moving

under a free surface were given in Bal (1999a) and Bal (1999b), respectively. On the other hand, emphasis is put on the Rankine panel methods both for 2-D and 3-D problems in this paper. One of the very important numerical solution methods that employed a distribution of Rankine type of sources on the ship hull and free surface was introduced by Dawson (1977). This method has increased in popularity since then and been applied to a wide range of ships. Nakos and Sclavounos (1994), however, computed steady wave patterns and wave resistance of several ship hulls, including transom-stern ships by a new Rankine panel method. The fundamental numerical attributes of this method were studied in Nakos and Sclavounos (1990). Another numerical method based on Rankine sources has been developed for the prediction of flow passing ships in Rigby et al. (2001). A desingularized boundary integral method for fully nonlinear free surface problems was described in Cao et al. (1991). An iterative boundary element (Rankine panel) method to solve the flow around surface piercing hydrofoils and ships was presented in Hsin and Chou (1998).

In the present study, however, the iterative boundary element method (IBEM) given in Bal et al. (2001) and Bal and Kinnas (2002) is first applied to a 2-D hydrofoil with an angle of attack. This IBEM allows the solution of the 2-D hydrofoil (body) problem and the free surface problem separately, with the effects of one problem on the other accounted for by the values of induced potential. The 2-D hydrofoil is modeled with constant strength dipole and constant strength source panels, distributed over the hydrofoil wetted surface. Details of the present low-order potential-based panel method can be found in Brebbia et al. (1984) and Kinnas and Fine (1993). The free surface is also modeled with constant strength dipole and constant strength source panels. The source strengths on the free surface are expressed by using the free surface condition, in terms of the second derivative of perturbation potential with respect to the horizontal axis. The corresponding second-order derivative is calculated by applying Dawson's fourth-order backward finite difference scheme (refer to Dawson (1977) and Bal (2008)). Then an integral equation for unknown perturbation potential values on the free surface is obtained by applying Green's theorem. The potential induced by the 2-D hydrofoil surface on the free surface and the potential induced by the free surface on the 2-D hydrofoil surface are considered on the right-hand sides of cor-

responding integral equations. To prevent upstream waves, the first- and second-order derivatives of perturbation potential with respect to horizontal axis are enforced to be equal to zero on the free surface (Nakos and Sclavounos, 1990). In order to achieve this, the source strengths on the free surface from a distance in front of the 2-D hydrofoil to the end of the truncated upstream boundary are enforced to be equal to zero. No radiation condition is enforced at the transverse and downstream boundaries (Nakos and Sclavounos, 1994). The present IBEM is first validated in the case of a constant strength point vortex and then applied to a NACA0012 hydrofoil with 5 degrees angle of attack. The effects of Froude number and the depth of submergence of the hydrofoil from the free surface on pressure distribution, lift and wave drag values, and the wave elevation are discussed. Then, the original method of Dawson is applied to predict the wave pattern and wave drag values of surface piercing bodies (ship hulls) or fully submerged bodies (submarine type of bodies) in the case of 3-D. Some extensive numerical results are also shown to compare with those of experiments and other numerical methods in the literature.

Mathematical Formulation of the Problem

2-D Problem

A fully submerged 2-D hydrofoil with an angle of attack is subjected to a uniform inflow (U), as shown in Figure 1. The x -axis is positive in the direction of uniform inflow (U), the z -axis is positive upwards, and the undisturbed free surface is located at $z = h$. The fluid (flow) is assumed to be inviscid, incompressible, and irrotational. Formulation of this problem is given in Bal et al. (2001) in detail. For completeness, it is summarized here as follows: Perturbation potential, ϕ , and total potential, Φ , should satisfy Laplace's equation in the fluid domain,

$$\nabla^2 \Phi = \nabla^2 \phi = 0 \quad (1)$$

Following boundary conditions should also be satisfied by perturbation potential ϕ as follows:

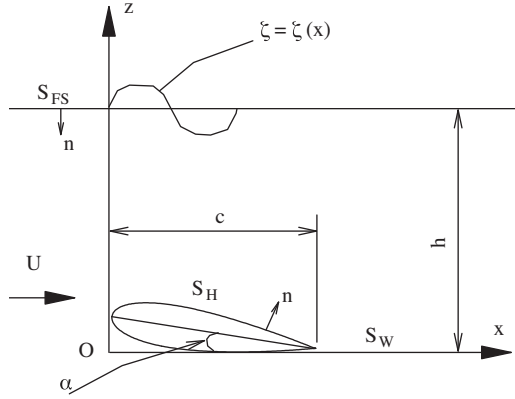


Figure 1. Definition of coordinate system for 2-D problem.

i) Kinematic boundary condition on the hydrofoil surface on S_H : The flow should be tangent to the wetted surface of the hydrofoil,

$$\frac{\partial \phi}{\partial n} = -\vec{U} \cdot \vec{n} \quad (2)$$

where \vec{n} is the unit normal vector to the wetted surface of the body, directed into the fluid domain, as shown in Figure 1.

ii) Kinematic free surface condition on S_{FS} : The fluid particles should follow the free surface,

$$\frac{DF(x, z)}{Dt} = 0 \quad \text{on } z = \zeta(x) + h \quad (3)$$

where $F(x, z) = z - \zeta(x)$, ζ the free surface deformation, see Figure 1.

iii) Dynamic free surface condition on S_{FS} : The pressure on the free surface should be equal to the atmospheric pressure (p_{atm}). Applying Bernoulli's equation, the following equation can be obtained:

$$\frac{1}{2} [(\nabla \Phi)^2 - U^2] + g\zeta = 0 \quad \text{on } z = \zeta(x) + h \quad (4)$$

where g is the gravitational acceleration.

If Eq. (3) and Eq. (4) are combined and linearized, then the following free surface condition can be derived:

$$\frac{\partial^2 \phi}{\partial x^2} + k_0 \frac{\partial \phi}{\partial z} = 0 \quad \text{on } z = h \quad (5)$$

Here, $k_0 = g/U^2$ is the wave number and the corresponding wave elevation can also be given as

$$\zeta = -\frac{U}{g} \frac{\partial \phi}{\partial x} \quad (6)$$

iv) Radiation condition on S_{FS} : No upstream waves should occur. In order to prevent upstream waves, both the first- and second-order derivatives of perturbation potential with respect to x are forced to be equal to zero for the upstream region on the free surface,

$$\frac{\partial^2 \phi}{\partial x^2} = \frac{\partial \phi}{\partial x} = 0 \quad \text{as } x \rightarrow -\infty \quad (7)$$

The origin and the physical interpretations of these 2 upstream conditions were discussed in more detail in Nakos and Scлавounos (1994).

v) Infinite depth condition: The perturbation potential should go to zero for infinite depth,

$$\lim_{z \rightarrow -\infty} \nabla \phi \rightarrow 0 \quad (8)$$

vi) Kutta condition: The velocity at the trailing edge of the hydrofoil should be finite,

$$\nabla \phi = \text{finite; at the trailing edge} \quad (9)$$

3-D Problem

A fully submerged 3-D body (submarine) or a surface piercing body (ship hull) is subjected to a uniform inflow (U), as shown in Figure 2. The x -axis is positive in the direction of uniform inflow, the z -axis is positive upwards, and the y -axis completes the right-handed system. The undisturbed free surface is located at $z = 0$. The fluid (flow) is assumed to be inviscid, incompressible, and irrotational. Formulation of this problem is given in Dawson (1977) in great detail. For completeness, a very brief summary is given here as follows:;The perturbation potential should satisfy the Laplace equation, Eq. (1), the kinematic body condition, Eq. (2), and the infinite depth condition, Eq. (8), similar to the above 2-D problem. The free surface condition, on the other hand, can be linearized by the double-model velocity potential (the potential of body itself + the potential of its mirror image with respect to free surface) $\phi(x, y, z)$ as

$$(\phi_l^2 \Phi_l)_l + g\Phi_z = 2\Phi_u \phi_l^2 \quad (10)$$

where $\Phi(x, y, z)$ is the total velocity potential and l is the streamline direction of the double-model solution on the undisturbed free surface $z = 0$ (refer to Dawson (1977) for details).

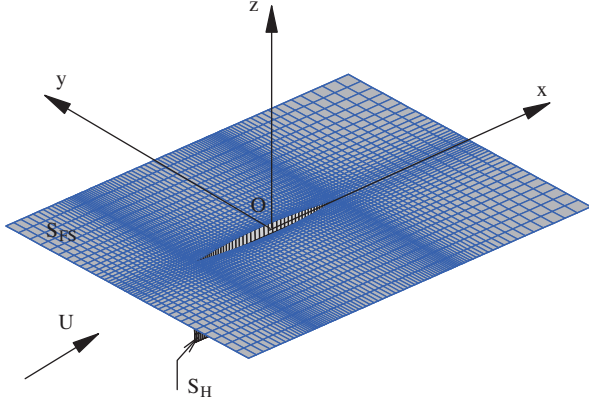


Figure 2. Definition of coordinate system in 3-D problem.

Numerical Formulation

2-D Problem

According to Green's third identity the perturbation potential on the hydrofoil surface and on the free surface can be expressed as

$$2\pi\phi = \int_{S_{FS}+S_H} \left(\phi \frac{\partial G}{\partial n} - \frac{\partial \phi}{\partial n} G \right) dS + \int_{S_W} \Delta\phi_W \frac{\partial G}{\partial n^+} dS \quad (11)$$

where S_H , S_W , and S_{FS} are the boundaries of the hydrofoil, wake, and the free surface, respectively. G is the Green function ($G = \ln r$). $\Delta\phi_W$ is the potential jump across the wake surface and n^+ is the unit vector normal to the wake surface pointing upwards. The wake surface leaving the trailing edge of the hydrofoil is located on the $z = 0$ plane (see Figure 1). In the present study, the iterative method developed in Bal et al. (2001) and Bal and Kinnaas (2002) is applied to solve Eq. (11). The iterative method here is composed of 2 parts: (i) the hydrofoil part, which solves for the unknown perturbation potential on S_H , and (ii) the free surface part, which solves for the unknown perturbation potential on S_{FS} . Potential in the fluid domain due to the influence of hydrofoil, ϕ_H , can be given as

$$2\pi\phi_H = \int_{S_H} \left(\phi \frac{\partial G}{\partial n} - \frac{\partial \phi}{\partial n} G \right) dS + \int_{S_W} \Delta\phi_W \frac{\partial G}{\partial n^+} dS \quad (12)$$

Potential in the fluid domain due to the influence of free surface, ϕ_{FS} , however, can also be given as

$$2\pi\phi_{FS} = \int_{S_{FS}} \left(\phi \frac{\partial G}{\partial n} - \frac{\partial \phi}{\partial n} G \right) dS \quad (13)$$

By substituting Eq. (13) into Eq. (11) and after applying the kinematic boundary condition, Eq. (2), the following integral equation for the flow on the hydrofoil can be derived as

$$2\pi\phi = \int_{S_H} \left(\phi \frac{\partial G}{\partial n} + (\vec{U} \cdot \vec{n}) G \right) dS + \int_{S_W} \Delta\phi_W \frac{\partial G}{\partial n^+} dS + 4\pi\phi_{FS} \quad (14)$$

and by substituting Eq. (12) into Eq. (11) and applying the linearized free surface condition, Eq. (5), similarly, the following integral equation for the flow on the free surface can be derived as

$$2\pi\phi = \int_{S_{FS}} \left(\phi \frac{\partial G}{\partial n} + \frac{1}{k_0} \frac{\partial^2 \phi}{\partial x^2} G \right) dS + 4\pi\phi_H \quad (15)$$

Integral Eqs. (14) and (15) can be solved iteratively by a low-order panel method with the potentials ϕ_H and ϕ_{FS} being updated during the iterative process. The hydrofoil surface, Eq. (14), and the free surface, Eq. (15), are discretized into straight panels with constant strength source and dipole distributions. The discretized integral equations provide 2 matrix equations (for the hydrofoil surface and for the free surface) with respect to the unknown potential values. In Eq. (15), the second-order derivative of perturbation potentials with respect to x is calculated by applying Dawson's original fourth-order backward finite difference scheme (Dawson, 1977). In order to prevent upstream waves, the first- and second-order derivatives of perturbation potential ϕ with respect to x are enforced to be equal to zero (Nakos and Sclavounos, 1990). It is assumed that the source strengths from some distance in front of the ship hull to the upstream truncation boundary on the free surface are equal to zero and result in $\frac{\partial \phi}{\partial z}$ being zero.

3-D Problem

For 3-D problems, quadrilateral panels are used in place of the straight panels of 2-D problems. The integrals over each panel are evaluated as described

by Hess and Smith (1966). According to Hess and Smith (1966), the wetted surface of the ship-hull (in the case of a surface piercing body) or submarine (in the case of a fully submerged body) is discretized into quadrilateral elements with constant source strengths. The basic expression for the potential flow around a double-model can be given as

$$\Phi(x, y, z) = \iint_S \frac{\sigma(q)}{r(p, q)} dS \quad (16)$$

where σ is the source density or strength, and r is the radial distance of the collocation or field point $p(x, y, z)$ from the integration control point $q(x, y, z)$. The integration domain S consists of the double-body model and the local free-surface region, which is covered by the Rankine source panels. More details of the method can be found in Dawson (1977).

Validation and Numerical Results

2-D Results

First, a point vortex with constant strength, $\Gamma/2\pi = 0.25 \text{ m}^2/\text{s}$ ($= 2.7 \text{ ft}^2/\text{s}$), is chosen to validate the present method in terms of Dawson's method (Dawson, 1977). The uniform flow velocity is $U = 3.048 \text{ m/s}$ ($= 10 \text{ ft/s}$) and the submergence depth of the point vortex is $h = 1.37 \text{ m}$ ($= 4.5 \text{ ft}$), and so it is possible to compare the wave elevations with those of Dawson's method. In Figure 3, the wave elevations of Dawson's method and the present method are shown. A satisfactory agreement is obtained. Here, in the application of Dawson's method, the strengths of imaginary straight source panels are assumed to be equal to zero. Note that no unrealistic upstream waves occur for Dawson's method and the wave heights are also in good agreement with those of the present method. The wave elevations calculated by the present method were compared with those of analytical ones in Bal et al. (2001). The agreement was excellent. The number of straight panels used on the free surface is here kept fixed, $\text{NFS} = 300$, for both Dawson's method and the present method.

Second, a fully submerged NACA0012 hydrofoil with angle of attack $\alpha = 5^\circ$ is chosen. The wave elevation, lift, and wave drag values of this hydrofoil were compared with those of experiments in Bal and Kinnas (2002). Here, some extensive results are shown. In Figure 4, the effect of Froude number ($\text{Fc} = U/(gc)^{0.5}$; c : chord of hydrofoil) on non-dimensional pressure distribution ($C_p = p/(0.5\rho U^2)$;

ρ : density of fluid) is shown for fixed ratio of submergence depth to chord, $h/c = 1.0$. The pressure distribution for unbounded flow domain (no free surface effect) is also added to Figure 4. Note that, while the case of $\text{Fc} = 0.5$ causes an increase in negative non-dimensional pressure distribution on the suction side of the hydrofoil, the cases of $\text{Fc} = 1.0$ and 1.5 cause a decrease with respect to the non-dimensional pressure distribution of unbounded flow domain. In Figure 5, the effect of submergence depth ratio (h/c) on non-dimensional pressure distribution is shown for a fixed Froude number, $\text{Fc} = 1.0$. The pressure distribution for unbounded flow domain (no free surface effect) is also added to Figure 5. Note that the pressure distribution is converging to those of unbounded flow domain for increasing h/c ratios. In Figure 6, the non-dimensional lift coefficient ($C_L = L/(0.5\rho c U^2)$; L : actual lift of hydrofoil) and non-dimensional wave drag coefficient ($C_D = D/(0.5\rho c U^2)$; D : actual wave drag of hydrofoil) values are given for different Fc numbers and h/c ratios. The unbounded flow domain lift values and wave drag values are also added to the same Figure 6. On the other hand, the effects of Fc number and h/c ratios on wave elevations are shown in Figures 7 and 8, respectively. It should be noted that increasing Fc numbers cause an increase in wave height and wave length while increasing h/c ratios cause only a decreasing wave height. The numbers of panels used on both the hydrofoil surface and the free surface are equal to each other and $\text{NFOIL} = \text{NFS} = 300$ for the calculations above.

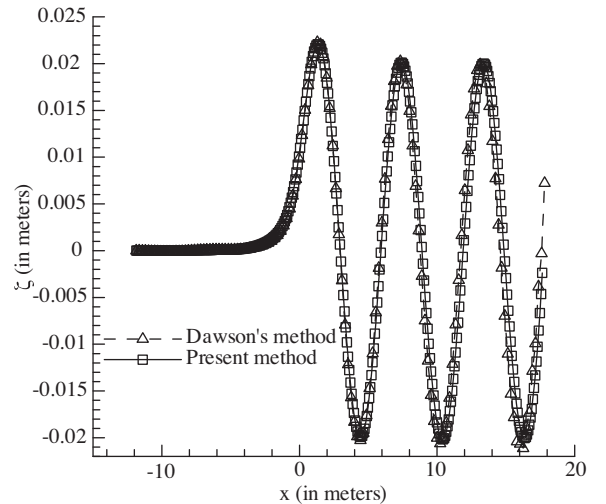


Figure 3. Wave elevations on free surface for constant strength point vortex.

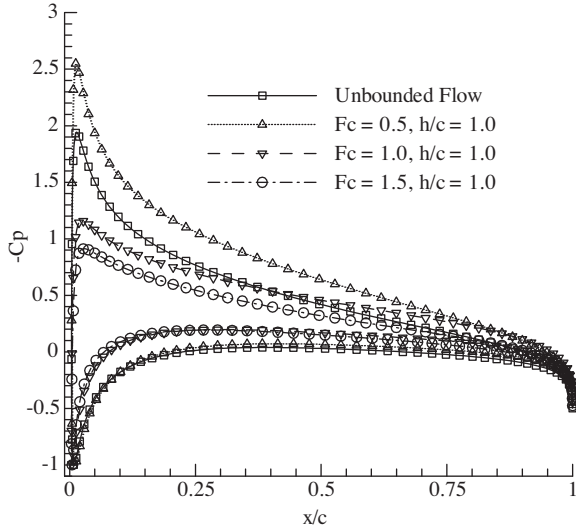


Figure 4. Froude number effect on pressure distribution for fixed submergence depth ratios.

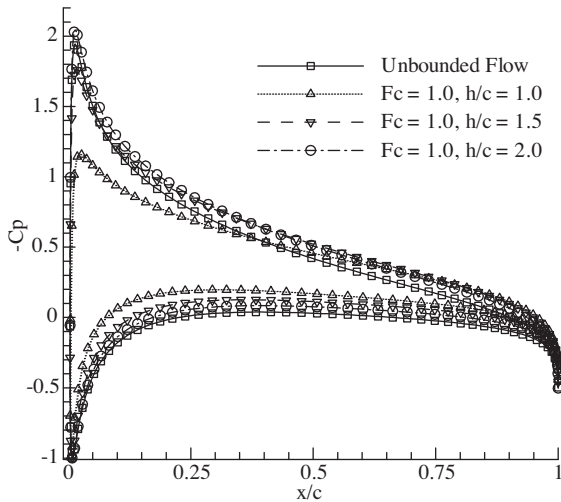


Figure 5. Submergence depth effect on pressure distribution for fixed Froude number.

3-D Results

First, a submerged axisymmetric ellipsoid is chosen to compare the results with those of another numerical method given in Farrell (1973). The perspective view of the panels used on both the ellipsoid surface and the free surface is illustrated in Figure 9. NXFS = 100, NYFS = 20 (total number of panels on the free surface is NFS = 100 × 20 = 2000), NXH = 90, NTH = 20 (total number of panels on the hull surface NHULL = 2 × 90 × 20 = 3600) are used for all calculations performed for the ellipsoid surface. The wave contours and wave deformations on

the free surface for Froude numbers ($Fn = \frac{U}{\sqrt{2ga}}$) = 0.4 and 0.8 are shown in Figures 10 and 11, respectively. The ellipsoid is between $-6 < x < 6$ in the corresponding Figures 10 and 11. Note that the lengths are increasing for increasing Froude numbers. In Figure 12, the effect of the free surface on pressure distribution is shown for $Fn = 0.8$ as compared with that of unbounded flow domain (no free surface effect). In Figure 13, the wave drag values (as defined by Farrell (1973)) for ellipsoids with different aspect ratios ($a/b = 4.5, 6.0, \text{ and } 8.0$; aspect ratio is defined as the ratio of length of the ellipsoid to the diameter) are given as compared with those of another numerical method in Farrell (1973). It should be noted that the agreement between the 2 methods is satisfactory.

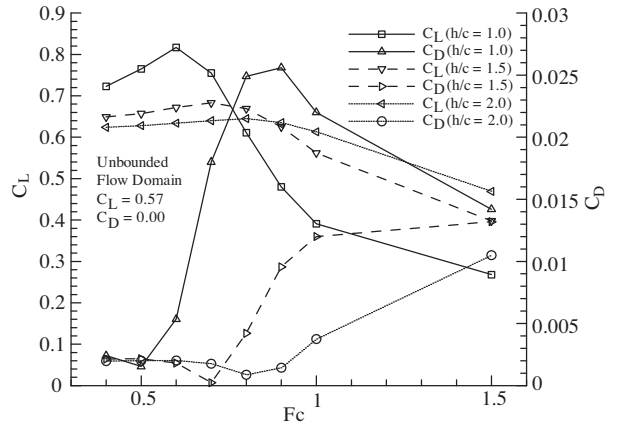


Figure 6. Froude number and submergence depth effect on lift and wave drag values.

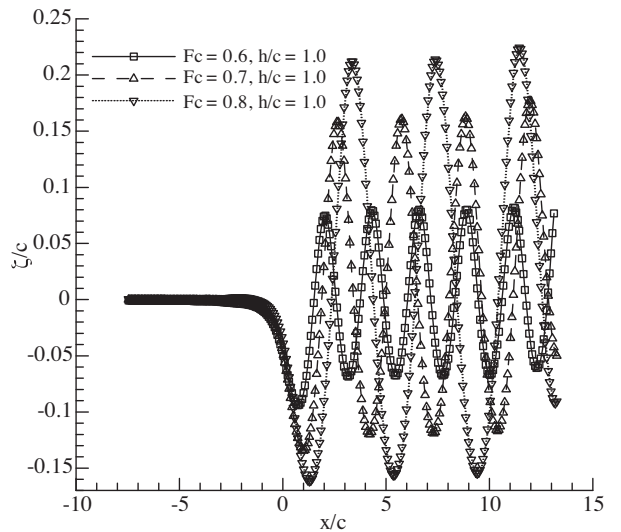


Figure 7. Froude number effect on wave elevation for fixed ratio of submergence depth to chord.

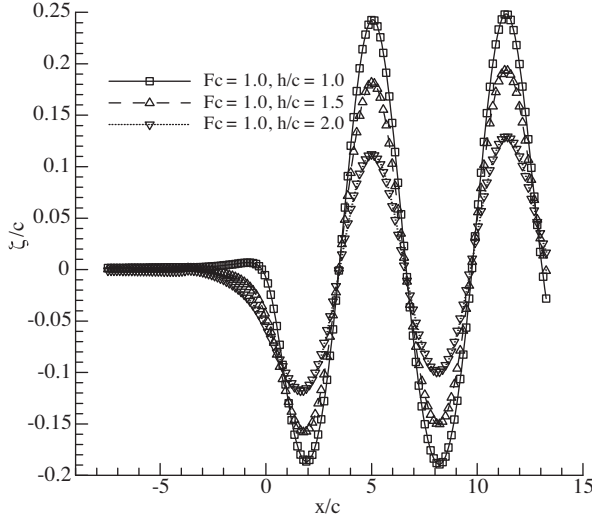


Figure 8. Submergence depth effect on wave elevation for fixed Froude number.

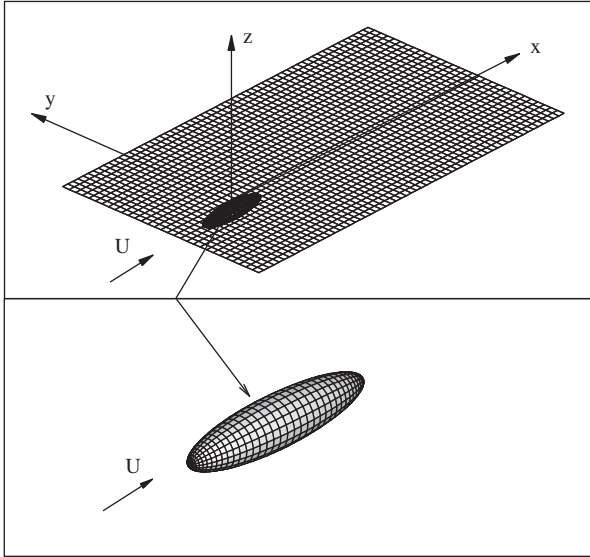


Figure 9. Panel arrangements on free surface (top) and on spheroid surface (bottom).

Second, Dawson's method is applied to a Wigley hull to validate it using measurements. The chosen hull has a length-to-beam ratio of 10 and a beam-to-draft ratio of 1.6 and the following equation for the hull surface:

$$y = \pm \frac{B}{2} \left[1 - \left(\frac{2x}{L} \right)^2 \right] \left[1 - \left(\frac{z}{H} \right)^2 \right] \quad (17)$$

where L is the length, B is the beam, and H is the draft. $NXFS = 100$, $NYFS = 20$ (total number of panels on the free surface is $NFS = 100 \times 20 =$

2000), $NXH = 90$, $NYH = 20$ (total number of panels on the hull surface $NHULL = 3600$) are used for all calculations performed for the Wigley hull. The wave contours and wave deformations on the free surface for Froude numbers ($Fn = \frac{U}{\sqrt{gL}}$) = 0.3 and 0.4 are shown in Figures 14 and 15, respectively. The wave contours for $Fn = 0.3$ and 0.4 taken from Bal (2008) are also illustrated to compare the results of the present Dawson's method with those of Bal (2008) in Figures 16 and 17, respectively. Note that the wave contours are consistent with those

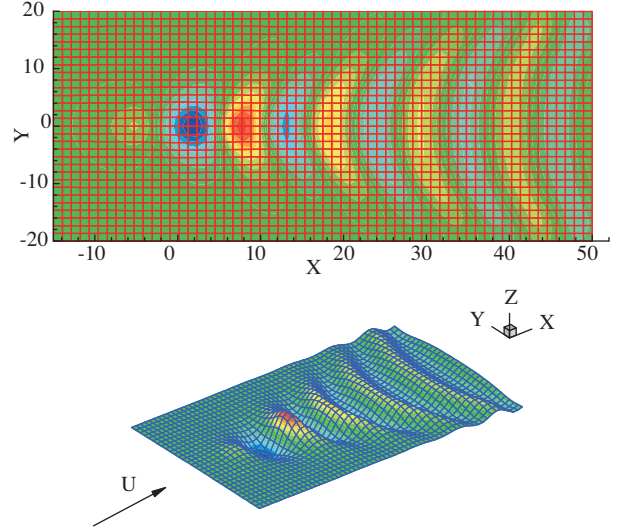


Figure 10. Wave contours and wave deformations for fully submerged ellipsoid for $Fn = 0.4$.

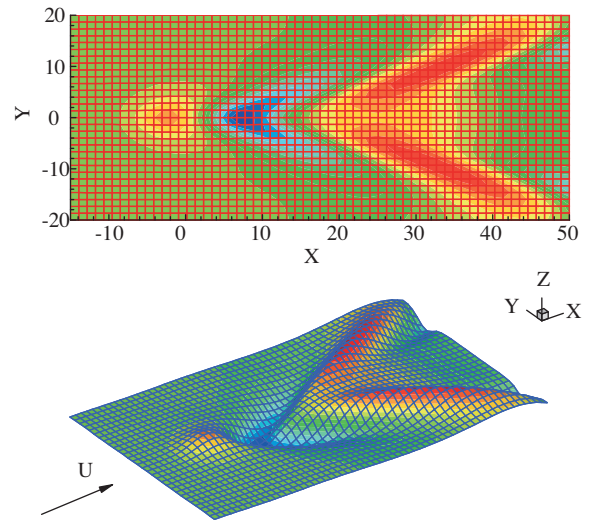


Figure 11. Wave contours and wave deformations for fully submerged ellipsoid for $Fn = 0.8$.

given by Bal (2008) and show compatible variation with respect to Froude number. In Figure 18, the pressure distribution on the Wigley hull is given as compared with that of unbounded flow domain. In Figure 19, the predicted values of wave resistance by the pressure integration on the hull surface are compared with those of experiments (model fixed case) and the linear method given by Nakos and

Sclavounos (1994). Although the wave drag values are higher for low Froude numbers ($F_n < 0.35$) than those of experiments, the agreement is satisfactory for higher Froude numbers and the wave drag curve shows compatible variation with respect to Froude number. The wave drag curve by Dawson's method is also consistent with the linear method given by Nakos and Sclavounos (1994).

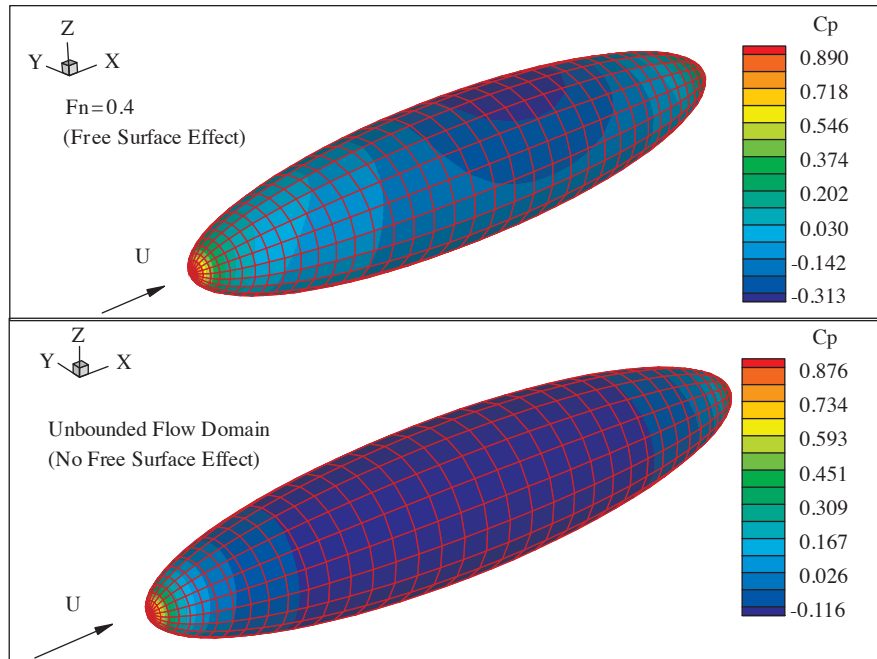


Figure 12. The non-dimensional pressure distribution on ellipsoid with free surface effect.

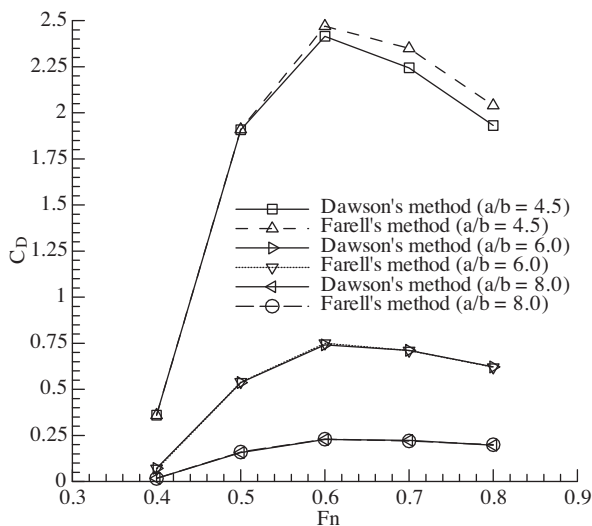


Figure 13. Wave drag values of ellipsoid with different aspect ratios.

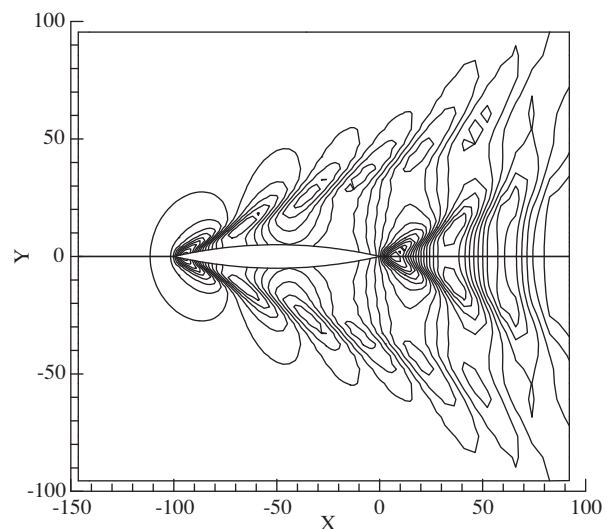


Figure 14. Wave contours of Wigley hull for $F_n = 0.3$ by Dawson's method.

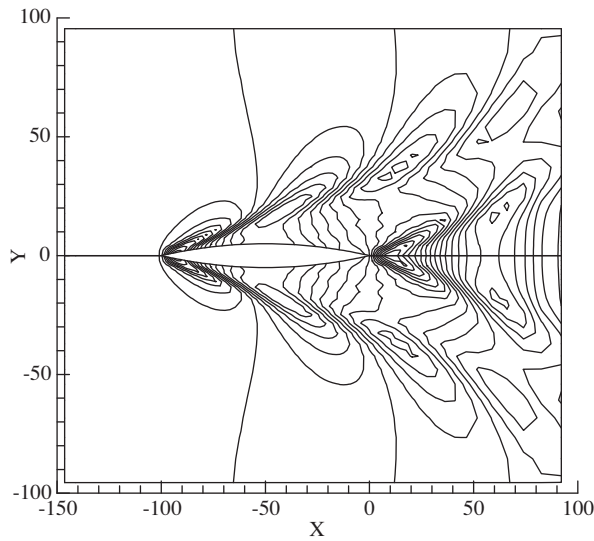


Figure 15. Wave contours of Wigley hull for $Fn = 0.4$ by Dawson's method.

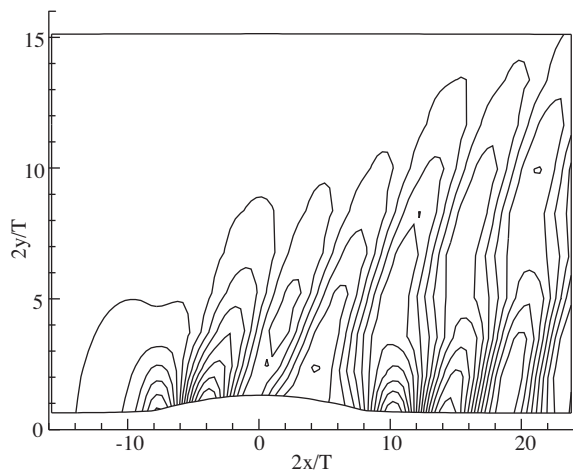


Figure 16. Wave contours of Wigley hull for $Fn = 0.3$, taken from Bal (2008).

Conclusions and Future Work

The wave drag, lift, wave pattern, and pressure distribution around 2-D and 3-D bodies moving with constant speed under or on a free surface are investigated by 2 different boundary element methods. The iterative boundary element method (IBEM), which is developed for 2-D and 3-D cavitating hydrofoils, is applied to a 2-D hydrofoil and some extended results are given. The effects of Froude number and the depth of submergence of the hydrofoil from the free

surface on pressure distribution lift and wave drag values and the free surface wave elevation are investigated. It is found that, while the Froude number $Fc = 0.5$ causes an increase in negative non-dimensional pressure distribution especially on the suction side of hydrofoil, the Froude numbers $Fc = 1.0$ and 1.5 cause a decrease with respect to the non-dimensional pressure distribution of unbounded flow domain. It is also found that the pressure distribution is converging to those of unbounded flow domain for increasing h/c ratios. In addition, it is shown that increasing Fc numbers cause an increase in wave height and wave length while increasing h/c ratios cause only a decreasing wave height.

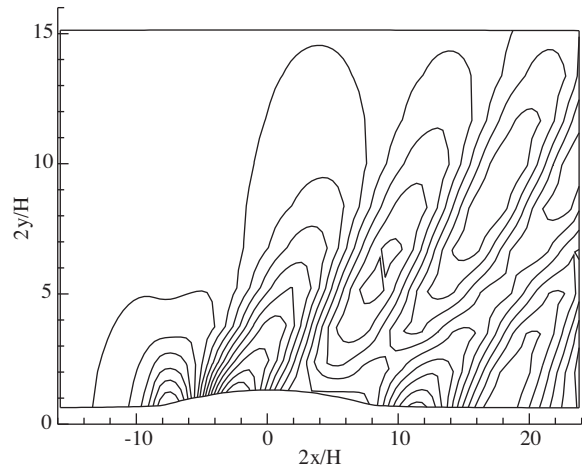


Figure 17. Wave contours of Wigley hull for $Fn = 0.4$, taken from Bal (2008).

The original method of Dawson, on the other hand, is applied to predict the wave pattern and wave drag values of surface piercing bodies (ship hulls) in the case of 3-D. Some extensive numerical results are also given as compared with those of experiments and other numerical methods in the literature so that a satisfactory agreement is obtained.

In the case of a 3-D ship hull (or submarine), an iterative boundary element method can be described in a similar way to that of the 2-D case given above by considering Dawson's algorithm and higher order effects of the free surface. The unsteady flow characteristics around a ship (or submarine) can also be included in the calculations by this corresponding 3-D IBEM.

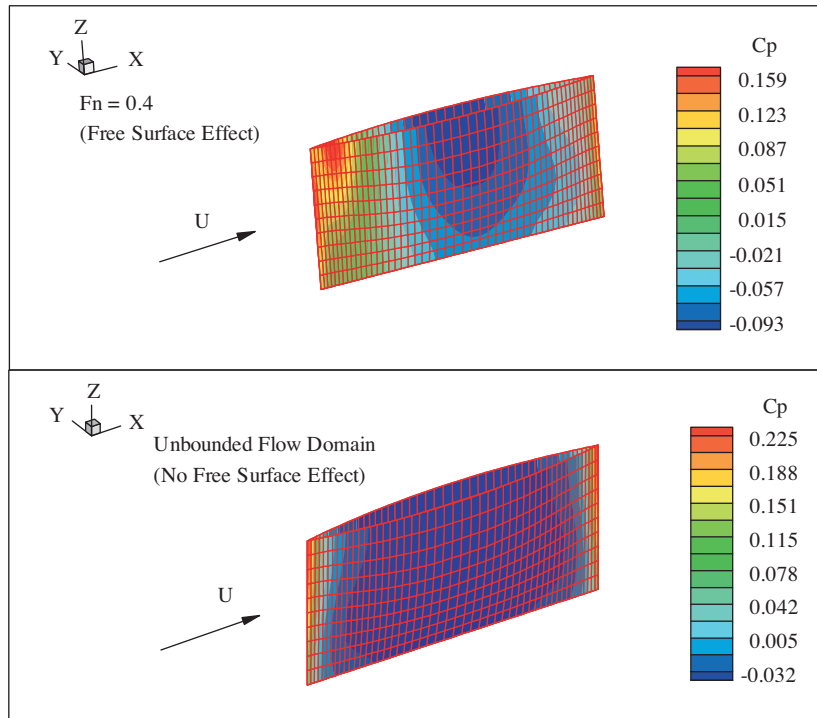


Figure 18. The non-dimensional pressure distribution on Wigley hull with free surface effect.

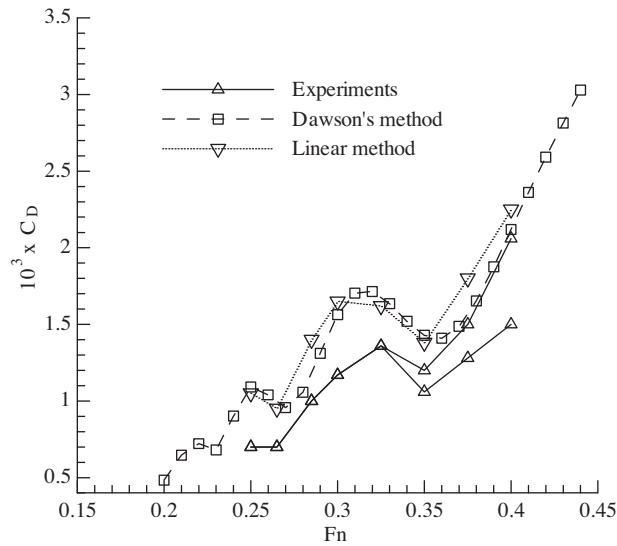


Figure 19. Wave drag values of Wigley hull.

Nomenclature

- | | | | |
|-----|-----------------------------|-------|--|
| a | half of length of ellipsoid | c | chord of hydrofoil |
| b | maximum radius of ellipsoid | C_D | wave drag coefficient of hydrofoil or ship |
| B | beam of ship (Wigley hull) | C_L | lift coefficient of hydrofoil |
| BEM | boundary element method | C_P | pressure coefficient |
| | | F_c | chord based Froude number, $F_c = U/(gc)^{0.5}$ |
| | | F_n | length based Froude number, $F_n = U/(gL)^{0.5}$ |

g	gravitational acceleration	S_{FS}	free surface
G	green function	S_H	hydrofoil or ship-hull surface
h	submergence depth of body from free surface	S_W	wake surface
IBEM	iterative boundary element method	T	draft of ship (Wigley hull)
k_0	wave number	U	velocity of uniform incoming flow
l	streamline direction of double-model solution in 3-D	α	angle of attack
L	length of ship (Wigley hull)	Φ	total potential
NFOIL	total number of panels on hydrofoil surface	ϕ	perturbation potential in 2-D or double-body potential in 3-D
NFS	total number of panels on free surface	ϕ_{FS}	induced potential by free surface on hydrofoil
NHULL	total number of panels on hull surface	ϕ_H	induced potential by hydrofoil on free surface
NTH	number of panels along tangential direction on ellipsoid	ρ	density of water
NXFS	number of panels along x direction on free surface	σ	source strengths
NYFS	number of panels along y direction on free surface	ζ	wave elevation
NXH	number panels along x direction on hull surface		
NZH	number panels along z direction on hull surface		
\vec{n}	unit normal vector directed from hydrofoil to water		
p	pressure value on body		
r	distance between source and control points		

Acknowledgments

This paper is a part of MSc thesis study by Yasin Uslu in the Department of Naval Architecture and Marine Engineering of İstanbul Technical University. The first author would like to thank Mr. Yaşar Gül, who is the Manager of DeltaMarine Design and Consultancy Company, for giving him the opportunity to perform this study.

References

- Bal, S., "A Potential-Based Panel Method for 2-D Hydrofoils", *Ocean Engineering*, 26, 343-361, 1999a.
- Bal, S., "A Panel Method for the Potential Flow around 2-D Hydrofoils", *Turkish J Eng Env Sci*, 23, 349-361, 1999b.
- Bal, S., "Prediction of Wave Pattern and Wave Resistance of Surface Piercing Bodies by a Boundary Element Method", *International Journal for Numerical Methods in Fluids*, 56, 305-329, 2008.
- Bal, S. and Kinnas, S.A., "A BEM for the Prediction of Free Surface Effects on Cavitating Hydrofoils", *Computational Mechanics*, 28, 260-274, 2002.
- Bal, S., Kinnas, S.A. and Lee H., "Numerical Analysis of 2-D and 3-D Cavitating Hydrofoils Under a Free Surface", *Journal of Ship Research*, 45, 34-49, 2001.
- Brebbia, C.A., Telles, J.C.F. and Wrobel, L.C., "Boundary Element Techniques - Theory and Applications in Engineering", Springer-Verlag, Berlin, 1984.
- Bulgarelli, U.P., Lugni, C. and Landrini, M., "Numerical Modeling of Free Surface Flows in Ship Hydrodynamics", *International Journal for Numerical Methods in Fluids*, 43, 465-481, 2003.
- Cao, Y., Schultz, W.W. and Beck, R.F., "Three-Dimensional Desingularized Boundary Integral Methods for Potential Problems", *International Journal for Numerical Methods in Fluids*, 12, 785-803, 1991.
- Dawson, D.W., "A Practical Computer Method for Solving Ship-Wave Problems", *Proc. 2nd Int. Conf. Numerical Ship Hydrodynamics*, Office of Naval Research, USA, 30-38, 1977.
- Farell, C., "On the Wave Resistance of a Submerged Spheroid", *Journal of Ship Research*, 17, 1-11, 1973.
- Hess, J.L. and Smith, A.M.O., "Calculation of Potential Flow About Arbitrary Bodies", *Progress in Aeronautical Science*, 8, 1966.
- Hsin, C.Y. and Chou, S.K., "Applications of a Hybrid Boundary Element Method to the Analysis of Free Surface Flow around Lifting and Nonlifting Bodies", *Proc. 22nd Symposium on Naval Hydrodynamics* Washington DC, USA, 129-138, 1998.
- Kinnas S.A. and Fine, N.E., "A Numerical Nonlinear Analysis of the Flow around Two- and Three-Dimensional Partially Cavitating Hydrofoils", *Journal of Fluid Mechanics*, 254, 151-181, 1993.

Nakos, D.E. and Slavounos, P.D., "On Steady and Unsteady Ship Wave Patterns", *Journal of Fluid Mechanics*, 215, 263-288, 1990.

Nakos, D.E. and Slavounos, P.D., "Kelvin Wakes and Wave Resistance of Cruiser- and Transom-Stern Ships", *Journal of Ship Research*, 38, 9-29, 1994.

Newman, J.N., "Marine Hydrodynamics", MIT Press, USA, 1977.

Rigby, S.G., Nicolaou, D., Sproston, J.L. and Millward, A., "Numerical Modeling of the Water Flow around Ship Hulls", *Journal of Ship Research*, 45, 85-94, 2001.

Tulin, M.P., "Reminiscences and Reflections: Ship Waves, 1950-2000". *Journal of Ship Research*, 49, 238-246, 2005.

Wehausen, J.V., "The Wave Resistance of Ships", *Advances in Applied Mechanics*, 13, 93-245, 1973.